Identification of post-pyrite phase transitions in SiO_{2} by a genetic algorithm

Shunqing Wu, Koichiro Umemoto, Min Ji, Cai-Zhuang Wang, Kai-Ming Ho, and Renata M. Wentzcovitch

Phys. Rev. B **83**, 184102 — Published 16 May 2011
DOI: 10.1103/PhysRevB.83.184102

Identification of post-pyrite phase transitions in SiO_2 by a genetic algorithm

Shunqing Wu[1,2], Koichiro Umemoto[3], Min Ji[1], Cai-Zhuang
Wang[1], Kai-Ming Ho[1], and Renata M. Wentzcovitch[4]
[1] *Ames Laboratory, US DOE and Department of Physics and Astronomy,*
Iowa State University, Ames, Iowa 50011, USA
[2] *Department of Physics, Xiamen University, Xiamen 361005, China*
[3]*Department of Geology and Geophysics,*
University of Minnesota, Minneapolis, MN 55455, USA
[4]*Minnesota Supercomputing Institute and Department*
of Chemical Engineering and Materials Science,
University of Minnesota, Minneapolis, MN 55455, USA

Abstract

Using a first-principles genetic algorithm we predict an Fe_2P phase is the first post-pyrite phase of SiO_2 at low temperatures. This contrasts with a recently predicted cotunnite phase. Static enthalpy differences between these two phases are small near the transition pressure (0.69 TPa). While quasiharmonic free energy calculations predict an Fe_2P-$\rightarrow$cotunnite-type transition with increasing temperature, another phase, NbCoB-type, is identified as being structurally and energetically intermediate between Fe_2P and cotunnite phases. This structure suggests a possible temperature-induced gradual transformation between Fe_2P and cotunnite phases. This finding would change our understanding of how planet-forming silicates, e.g. $MgSiO_3$ post-perovskite and its solid solutions, dissociate into elementary oxides at thermodynamic conditions expected in the interior of solar giants and exoplanets.

PACS numbers:

$MgSiO_3$ is a major constituent of Earth's mantle. The discovery of the post-perovskite (PPV) transition of $MgSiO_3$ near Earth's core-mantle boundary conditions [1–3] reminded us that minerals can have truly unexpected high-pressure behavior. This finding naturally introduced a new question: what is the next high pressure polymorph of $MgSiO_3$? The answer is fundamental for modeling the interiors of recently discovered exoplanets, particularly the terrestrial type [4, 5], and the cores of the solar giants, where pressures and temperatures can reach 4 TPa and 21,000 K [6]. In 2006, the dissociation of $MgSiO_3$ PPV into CsCl-type MgO and cotunnite-type SiO_2 was predicted at 1.1 TPa [7]. This prediction was based on the assumption of a sequence of pressure-induced transitions in SiO_2: rutile$\rightarrow$$CaCl_2$ $\rightarrow$$\alpha$-$PbO_2$ $\rightarrow$pyrite $\rightarrow$cotunnite phases. Experimentally, only phases up to pyrite-type SiO_2 have been observed to date [8]. This sequence of transitions seemed very reasonable because (i) MgF_2, a low-pressure analog of SiO_2, undergoes the same sequence of pressure-induced transitions from rutile up to pyrite and then transitions to the cotunnite phase [11] preceeded by phase X in a very narrow pressure range [12] and (ii) the cotunnite phase has cation coordination number (CN) higher (9) than that of the pyrite phase (6). Nevertheless, it is not guaranteed at all that the cotunnite phase is the real post-pyrite phase of SiO_2. The predicted transition pressure to the cotunnite phase, ~0.69 TPa [7, 13], is still too high to be observed in static compression experiments. Prediction of high-pressure phases in the multi-Mbar regime is a difficult problem and behavior of low-pressure analogs is often invoked. Comparison of enthalpies and/or Gibbs free energies of potential structures is the method frequently used (Refs. [13, 14] for postpyrite SiO_2) to predict phases at ultra-high pressures. However, these strategies do not guarantee that the true stable structure is identified. Structural search using genetic algorithms (GA) are much more likely to catch truly stable phases and this method has been proven to work very efficiently [15–17].

Here we show that a first-principles GA search predicts the Fe_2P phase as the first post-pyrite phase of SiO_2. The cotunnite phase has very competitive enthalpy but definitely higher than that of the Fe_2P phase beyond the stability field of the pyrite structure. However, the cotunnite phase is stable at high temperatures according to quasiharmonic (QHA) free energy calculations [28]. These two structures are very closely related, and the existence of another competitive and structurally intermediate phase, the NbCoB-type, suggests a gradual crossover between them. We also discuss the effect of these new phase transitions on the dissociation of $MgSiO_3$ PPV.

First-principles GA structural searches were performed at 0.5 and 2 TPa. The details of our GA algorithm were described elsewhere [17]. The number of structures in the GA pool was 32 or 64. The candidate structure pool was initially generated from experimentally-known and randomly-generated structures. We considered primitive cells with 1∼8 SiO_2 formula units (FUs). We used the local density approximation (LDA) [18, 19]. Two sets of silicon and oxygen pseudopotentials were generated by Vanderbilt's method [22]. For the GA searches, we used pseudopotentials generated using the following electronic configurations: $3s^2 3p^1 3d^0$ and $2s^2 2p^4$ with cutoff radii of 1.6 and 1.4 a.u. for silicon and oxygen, respectively. They required a cutoff energy of 40 Ry. Brillouin-zone integration was performed using the Monkhorst-Pack sampling scheme [23] over **k**-point meshes of spacing $2\pi \times 0.05\text{Å}^{-1}$. In the structure relaxation steps, constant-pressure variable-cell-shape molecular dynamics, [24, 25] was used. Candidate structures obtained with the GA were refined and their static enthalpies and QHA free energies were calculated using harder pseudopotentials, more suitable for the extreme pressures addressed here [7]. The valence electronic configurations of these harder pseudopotentials were $2s^2 2p^6 3s^1 3p^0$ and $2s^2 2p^4 3d^0$ with cutoff radii of 1.2 and 1.0 a.u. for silicon and oxygen, respectively. Their cutoff energy was 400 Ry. We used density-functional perturbation theory to compute dynamical matrices at $2 \times 2 \times 2$ **q**-point mesh for all phases [26, 27]. Phonon frequencies were then calculated by interpolation onto **q**-point meshes fine enough to achieve convergence of QHA free energy within 1 mRy/FU. All first-principles calculations were performed using the Quantum-ESPRESSO software distribution [29], which has been interfaced with the GA scheme in a fully paralleled manner.

The present GA scheme is quite efficient in this system at high pressure. It takes approximately ten generations at most to reach ground-state configurations for inspected cases. For instance, at 0.5 TPa, the GA search using 4-FU SiO_2 produces a pyrite ground-state in just a few generations, as shown in Fig. 1. At 2 TPa, for 4-FU SiO_2, the cotunnite structure is predicted to be the ground-state. For 3-FU SiO_2 at both 0.5 and 2 TPa, the Fe_2P structure is rapidly predicted. For 6-FU and 8-FU SiO_2, Fe_2P and cotunnite structures are predicted, respectively. These results indicate that Fe_2P and cotunnite phases are indeed good candidates for post-pyrite phases of SiO_2.

Fe_2P and cotunnite structures (Fig. 2) are closely related [30, 31]. Both have tricapped triangular prisms as structural units with silicon coordination number (CN) equal to 9 (=6+3). The lower-pressure phases of SiO_2 (rutile, $CaCl_2$, α-PbO_2, and pyrite) consist of

Si octahedra. In the α-PbO_2 structure, shifts of silicons from the octahedral center to the middle of an octahedral face give rise to tricapped triangular prisms [31]. If all silicons shift in the same direction, the α-PbO_2 structure transforms into the cotunnite structure. If half of silicons shift in the opposite direction, the α-PbO_2 structure changes into the Fe_2P structure. Several other structures with tricapped triangular prisms can be produced by different shifting patterns. Among them, the NbCoB structure, whose unit cell consists of 10 FUs [32], is worthy of note because it is intermediate between Fe_2P and cotunnite structures. In this structure, Fe_2P and cotunnite structures appear in an alternating pattern (Fig. 2). Therefore, the NbCoB phase is also a potential post-pyrite phase. Calculated structural parameters of these three potential post-pyrite phases of SiO_2 are given in Table I.

Several other phases appeared in GA pools. Among them, the Li_2ZrF_6 structure [33] is also worthy of note. This phase consists of silicon octahedra and is closely related with the α-PbO_2 structure [31], in the same way as Fe_2P and cotunnite structures are related. Fe_2P and cotunnite structures with tricapped triangular prisms are structural counterparts of Li_2ZrF_6 and α-PbO_2 structures with octahedra. Fe_2P-type SiO_2 can be obtained from Li_2ZrF_6-type by shifting all silicons in the same direction from octahedral centers to octahedral faces. Similarly to the NbCoB structure, there might be an intermediate phase between α-PbO_2 and Li_2ZrF_6 as well. At 2 TPa, most phases in GA pools, including the baddeleyite phase, are found to consist of capped triangular prisms. Enthalpy calculations with harder pseudopotentials confirm that these phases are metastable over the entire pressure range investigated here; Li_2ZrF_6-type SiO_2 has higher enthalpy than α-PbO_2-type at all pressures.

Figure 3 shows relative enthalpies of several phases of SiO_2. The PBE-type generalized gradient approximation [20] give rise to the same results as LDA essentially. Calculated transition pressures by PBE is higher by just ~10 GPa, as usually expected [21]. Static calculations show that pyrite-type SiO_2 transforms to Fe_2P-type at 0.69 TPa, being consistent with Ref. [14]. This transition pressure is almost identical to the metastable transition pressure between pyrite-type and cotunnite-type SiO_2. Although cotunnite and NbCoB phases are metastable over all pressures in static calculations, their enthalpies are very competitive. Below 0.64 TPa, the cotunnite phase has lower enthalpy than Fe_2P. Above 0.78 TPa, the NbCoB phase has intermediate enthalpy between those of Fe_2P and cotunnite phases. At 1 TPa, enthalpy differences between cotunnite and Fe_2P and between NbCoB and Fe_2P phases are just 0.006 Ry/FU and 0.004 Ry/FU. At 2 TPa, these differences increase to 0.017

Ry/FU and 0.01 Ry/FU (at most ∼3000 K). Phonon calculations show that all three phases are dynamically stable beyond ∼0.4 TPa.

Figure 4(a) shows the phase diagram of SiO_2 predicted by the QHA. Post-pyrite transitions to Fe_2P and cotunnite phases have negative Clapeyron slopes. This results from the increase in CNs and bond-lengths in Fe_2P and cotunnite phases, which increases density of states of low-frequency vibrations and vibrational entropies across these post-pyrite transitions [34]. In contrast, the phase boundary between Fe_2P and cotunnite phases has a normal positive Clapeyron slope. Below (above) ∼1500 K, pyrite-type SiO_2 should transform to a Fe_2P-type (cotunnite-type) SiO_2. In contrast, the NbCoB phase does not have a stability field. However, entropic stabilization of disordered structural motifs intermediate between Fe_2P and cotunnite is very likely at high temperatures. Therefore, the Fe_2P to cotunnite transition might not be sharp but a rather gradual transformation. Actually, the possibility that a fully disordered, mixed, or even dynamically-disordered phase is stable at high-temperatures cannot be discarded. However, the cotunnite phase is very stable without phonon instabilities in the pressure and temperature range of the phase diagram we presented, suggesting a crossover.

The presence of the Fe_2P phase introduces an additional phase boundary in the dissociation phase diagram of $MgSiO_3$ PPV as shown in Fig. 4(b). In the icy giants, Uranus and Neptune, the dissociation into MgO and SiO_2 should not occur. In the gas giants, Saturn and Jupiter, the dissociation into CsCl-type MgO and cotunnite-type SiO_2 occurs first. At higher pressures, depending on the internal temperature profiles in these planets, cotunnite-type SiO_2 might transform to Fe_2P-type. In GJ876d, a terrestrial exoplanet [35] with ∼7.5 Earth masses ($7.5M_\oplus$), conditions estimated at the core-mantle boundary [36] are close to the dissociation phase boundary.

Finally, the predicted structural crossover between Fe_2P and cotunnite phases should be fundamental to understanding the high-pressure and high-temperature behavior of AX_2-type compounds. Although pressures for the predicted phenomenon in SiO_2 are challenging to experiments, low-pressure analogs could be investigated to validate our predictions. MgF_2 is particularly suitable because it has a very similar sequence of phase transitions to SiO2. In combination with NaF it forms $NaMgF_3$ perovskite, that has the same sequence of predicted phase transitions as $MgSiO_3$ perovskite [7, 37], including dissociation into elementary fluorides/oxides. There are still unresolved questions in the experimental high-pressure behavior of $NaMgF_3$ and MgF_2 [12, 38]. The structural crossover between Fe_2P and cotunnite phases might be part of the answer.

Work at Ames Laboratory was supported by the US Department of Energy, Basic Energy Sciences, Division of Materials Science and Engineering, under Contract No. DE-AC02-07CH11358, including a grant of computer time at the National Energy Research Supercomputing Centre (NERSC) in Berkeley, CA. KU and RMW's work were supported by NSF grants EAR-0757903, EAR-0810272, EAR-1047629, and ATM-0426757 (VLab). Computations at the University of Minnesota were performed at the Minnesota Supercomputing Institute and at the Laboratory for Computational Science and Engineering. During the review process, a paper reporting the Fe_2P-type phase of SiO_2 by Tsuchiya and Tsuchiya was published [39].

---

[1] M. Murakami, K. Hirose, K. Kawamura, N. Sata, and Y. Ohishi, Science **304**, 855 (2004).

[2] A. R. Oganov and S. Ono, Nature **430**, 445 (2004).

[3] T. Tsuchiya, J. Tsuchiya, K. Umemoto, and R. M. Wentzcovitch, Earth Planet Sci. Lett. **224**, 241 (2004).

[4] A. P. van den Berg, D. A. Yuen, G. L. Beebe, and M. D. Christiansen, Phys. Earth Planet. Inter. **178**, 136 (2010).

[5] D. D. Sasselov and D. Valencia, Scientific American **303**, 38 (2010).

[6] T. Guillot, Physics Today **57**, 63 (2004).

[7] K. Umemoto, R. M. Wentzcovitch, and P. B. Allen, Science **311**, 983 (2006).

[8] Y. Kuwayama, K. Hirose, N. Sata, and Y. Ohishi, Science **309**, 923 (2005).

[9] R. M. Wentzcovitch, Y. Yu, Z. Wu, Rev. Mineral. Geochem. **71**, 99 (2010).

[10] D. Sasselov and D. Valencia, Scientific American **303**, 38 (2010).

[11] J. Haines, J. M. Leger, F. Gorelli, D. D. Klug, J. S. Tse, and Z. Q. Li, Phys. Rev. B **64**, 134110 (2001).

[12] B. Grocholski, S.-H. Shim, and V. B. Prakapenka, Geophys. Res. Lett. **37**, L14204 (2010).

[13] A. R. Oganov, M. J. Gillan, and G. D. Price, Phys. Rev. B **71**, 064104 (2005).

[14] T. Tsuchiya, J. Tsuchiya, A. Metsue, and T. Ishikawa, Acta Mineralogica-Petrographica, abstract series **6**, 810 (2010).

[15] A. R. Oganov and C. W. Glass, J. Chem. Phys. **124**, 244704 (2006).

[16] G. Trimarchi and A. Zunger, J. Phys.: Condens. Matter, **20**, 295212 (2008).

[17] M. Ji, C.-Z. Wang, and K.-M. Ho, Phys. Chem. Chem. Phys. **12**, 11617 (2010).

[18] D. M. Ceperley and B. J. Alder, Phys. Rev. Lett. **45**, 566 (1980).

[19] J. P. Perdew and A. Zunger, Phys. Rev. B **23**, 5048 (1981).

[20] J. P. Perdew, K. Burke, and M. Ernzerhof, Phys. Rev. Lett. **77**, 3865 (1996); **78**, 1396.

[21] R. M. Wentzcovitch, Y. Yu, and Z. Wu, Rev. Mineral. Geochem. **71**, 59 (2010).

[22] D. Vanderbilt, *Phys. Rev.* B **41**, R7892 (1990).

[23] H. J. Monkhorst and J. D. Pack, Phys. Rev. B **13**, 5188 (1976).

[24] R. M. Wentzcovitch, Phys. Rev. B **44**, 2358 (1991).

[25] R. M. Wentzcovitch, J. L. Martins, and G. D. Price, Phys. Rev. Lett. bf 70, 3947 (1993).

[26] S. Baroni, S. de Gironcoli, A. Dal Corso, and P. Giannozzi, Rev. Mod. Phys. **73**, 515 (2001).

[27] P. Giannozzi, S. de Gironcoli, P. Pavone, and S. Baroni, Phys. Rev. B **43**, 7231 (1991).

[28] D. Wallace, *Thermodynamics of Crystals* (Wiley, New York) (1972).

[29] P. Giannozzi et al., J. Phys.: Condens. Matter **21**, 395502 (2009).

[30] P. Dera, B. Lavina, L. A. Borkowski, V. B. Prakapenka, S. R. Sutton, M. L. Rivers, R. T. Downs, N. Z. Boctor, and C. T. Prewitt, Geophys. Res. Lett. **35**, L10301 (2008).

[31] B. G. Hyde and S. Andersson, *Inorganic Crystal Structures* (Wiley, New York) (1989).

[32] P. I. Krypyakevich, Y. B. Kuz'ma, Y. V. Voroshilov, C. B. Shoemaker, and D. P. Shoemaker, Acta Cryst. B**27**, 257 (1971).

[33] G. Brunton, Acta Cryst. B**29**, 2294 (1973).

[34] A. Navrotsky, Geophys. Res. Lett. **7**, 709 (1980).

[35] E. J. Rivera et al., Astrophys. J. **634**, 625 (2005).

[36] D. Valencia, R. J. O'Connell, and D. Sasselov, Icarus **181**, 545 (2006).

[37] K. Umemoto, R. M. Wentzcovitch, D. J. Weidner, and J. B. Parise, Geophys. Res. Lett. **33**, L15304 (2006).

[38] C. D. Martin, W. A. Crichton, H. Liu, V. Prakapenka, J. Chen, and J. B. Parise, Geophys. Res. Lett. **33**, L11305 (2006).

[39] T. Tsuchiya and J. Tsuchiya, Proc. Nat. Acad. Sci. **106**, 1252 (2011).

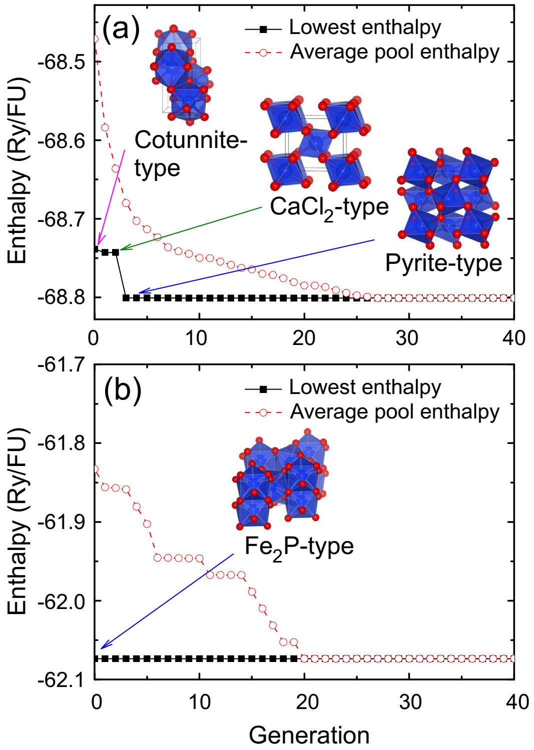

FIG. 1: The histories of the lowest energy (enthalpy) and the average pool energy (enthalpy) of (a) 4-FU at 0.5 TPa and (b) 3-FU SiO_2 at 2.0 TPa by generation.

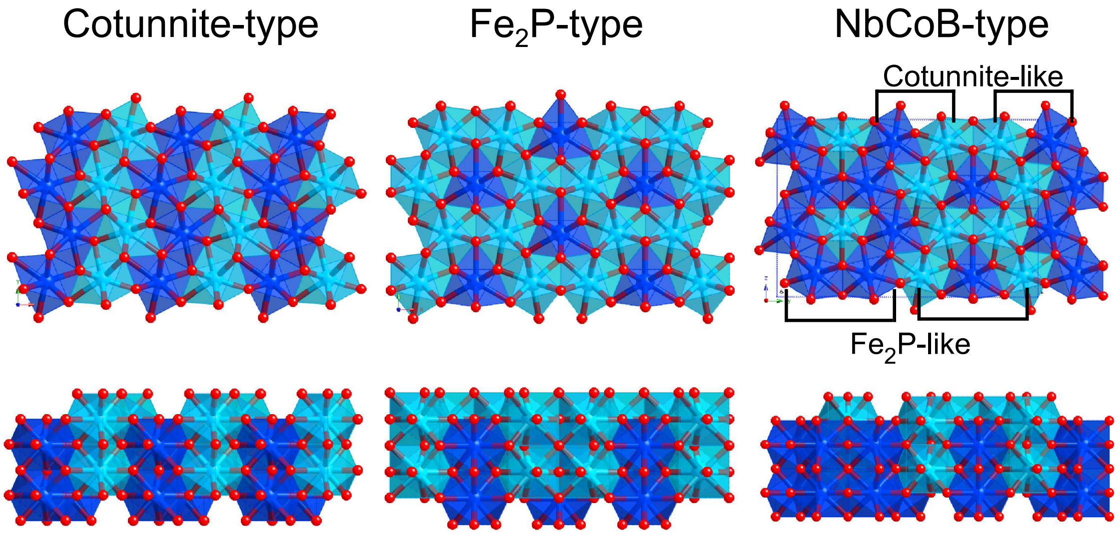

FIG. 2: Crystal structures of Fe_2P-, cotunnite- and NbCoB-type phases. Blue and light blue spheres denote silicon atoms at different heights. Red small spheres denote oxygen atoms.

Fe_2P-type SiO_2		
Space group		$P\bar{6}2m$
(a, c)		(4.120Å, 2.222Å)
Si_1	$2c$	(1/3, 2/3, 0)
Si_2	$1b$	(0, 0, 1/2)
O_1	$3f$	(0.2567, 0, 0)
O_2	$3g$	(0.5903, 0, 1/2)
(B, B')		(2.76 TPa, 2.71)
Cotuninte-type SiO_2		
Space group		$Pnma$
(a, b, c)		(4.108Å, 2.191Å, 4.853Å)
Si	$4c$	(0.2335, 1/4, 0.1387)
O_1	$4c$	(0.3472, 1/4, 0.4347)
O_2	$4c$	(0.9845, 1/4, 0.6670)
(B, B')		(2.75 TPa, 2.71)
NbCoB-type SiO_2		
Space group		$Pmmn$
(a, b, c)		(2.218Å, 12.010Å, 4.094Å)
Si_1	$4e$	(1/4, 0.4470, 0.7612)
Si_2	$4e$	(1/4, 0.3500, 0.2629)
Si_3	$2b$	(1/4, 3/4, 0.2375)
O_1	$4e$	(1/4, 0.5675, 0.5202)
O_2	$4e$	(1/4, 0.6287, 0.025)
O_3	$2b$	(1/4, 3/4, 0.6454)
O_4	$4e$	(1/4, 0.4722, 0.1542)
O_5	$4e$	(1/4, 0.3270, 0.6330)
O_6	$2a$	(1/4, 1/4, 0.0198)
(B, B')		(2.75 TPa, 2.71)

TABLE I: Structural parameters of Fe_2P-, cotunnite-, and NbCoB-type SiO_2 at 0.8 TPa. Bulk modulus (B) and its pressure derivative (B') at 0.8 TPa were obtained by the third-order Birch-Murnaghan equation of states.

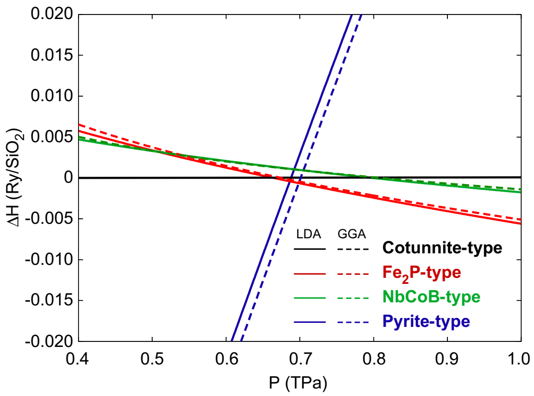

FIG. 3: Enthalpies of pyrite-, Fe_2P-, and NbCoB-type SiO_2 with respect to cotunnite-type SiO_2.

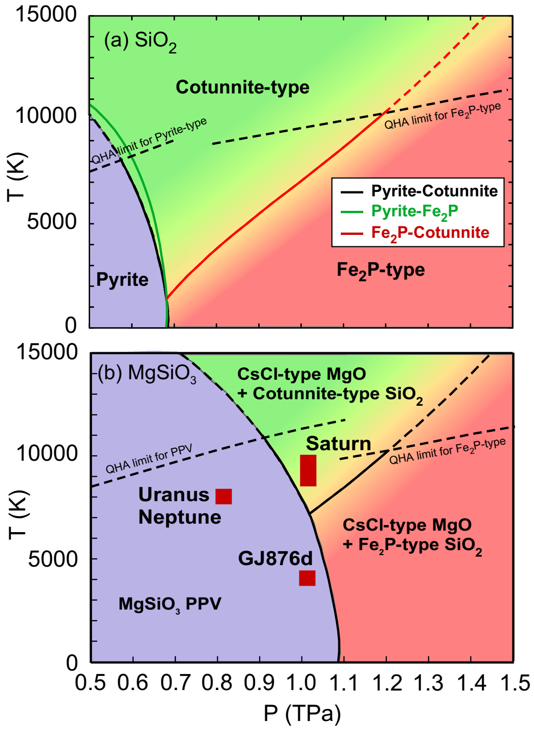

FIG. 4: Pressure-temperature phase diagram of (a) SiO_2 and (b) dissociation of $MgSiO_3$ PPV into MgO and SiO_2. Free energy of $MgSiO_3$ PPV published in Ref. [7] is used. The transformation between Fe_2P- and cotunnite-type SiO_2 is expected to be gradual (see text). Red areas denote estimated pressure-temperature conditions at core-envelope boundaries in the solar giants [6] and in the GJ876d [36]. Dashed lines indicate the limit of validity of the QHA.